Demonstration of Tunable Fano Resonances In A Meta-Material Absorber Composed of Asymmetric Double Bars With Bent Arms

Aliakbar Mashkour
Islamic Azad University
Amangaldi Koochaki (koochaki@aliabadiau.ac.ir)
Islamic Azad University https://orcid.org/0000-0001-6841-534X
Ali Abdolahzadeh Ziabari
Islamic Azad University
Azadeh Sadat Naeimi
Islamic Azad University

Research Article

Keywords: MIM, Plasmonic, Absorber, Fano, Dipole

Posted Date: July 9th, 2021

DOI: https://doi.org/10.21203/rs.3.rs-663879/v1

Demonstration of Tunable Fano Resonances in a Meta-Material Absorber Composed of Asymmetric Double Bars with Bent Arms

Aliakbar Mashkour[1], Amangaldi Koochaki[1,*], Ali Abdolahzadeh Ziabari[2], Azadeh Sadat Naeimi[3]

[1] *Department of Electrical Engineering, Aliabad Katoul Branch, Islamic Azad University, Aliabad Katoul, Iran*

[2] *Nano Research Lab, Lahijan Branch, Islamic Azad University, Lahijan, Iran*

[3] *Department of Physics, Aliabad Katoul Branch, Islamic Azad University, Aliabad Katoul, Iran*

Abstract:

In this paper a Metal-Insulator-Metal (MIM) plasmonic absorber consisting of asymmetric double bars with bent arms located on top of a silica layer coated on a metal film is proposed, and its resonant features are analyzed. The suggested structure supports both Fano and dipole perfect absorption resonances at the Near-Infrared Region (NIR). The asymmetry introduced into the structure can be induced by changing the bending angle or rotation angle of one of the antennas while the other one remains fixed. Simulation results demonstrate that by applying both asymmetry factors to the structure, one can have two individual Fano peaks at the same time. It is shown that the magnitude, central wavelength and line-width of the Fano peaks are adjustable by controlling the geometrical parameters of the structure. It is also indicated that, the quality factor (Q-factor) of the Fano resonance is inversely related to the degree of asymmetry introduced into the structure. According to the simulations, an ultra-narrow resonance peak with a bandwidth of 1.87 nm at the wavelength of 710 nm (corresponding to a Q-factor of 387) can be obtained by controlling the geometrical parameters. It is also discussed that, the absorptivity of Fano and the dipole peaks can be adjusted inversely, by manipulating the grapheme chemical potential. The ratio of the absorptivity to the chemical potential of graphene about-275 %/eV and 226 %/eV is calculated for the Fano peak and dipole peak, respectively. Accordingly, the presented structure is an adjustable NIR absorber with a fully tunable absorption spectrum which can be utilized in various applications from tunable reflectors and photo-detectors to ultra-narrowband and broadband optical modulators.

Keywords: MIM, Plasmonic, Absorber, Fano, Dipole

1. Introduction:

During the recent decades, the efficient tunability of the optical spectrum of meta-material absorbers have intensely attracted the attention of many researchers, since they play a key role in a wide range of applications including tunable optical filters [1-3], nano-sensors [4, 5], photo-detectors [6-8],optical switches, and so on. This efficient tunability stems from the efficiently adjustable Electro-Magnetic (EM) field strengths associated with resonant excitation of plasmons inside the metallic nano-structures[9].

Several efforts have so far been devoted to improve the performance of meta-material absorbers in terms of absorption efficiency. This is realizable through enhancement of the intensity of their electromagnetic plasmon fields at the desired wavelengths. Two typical methods have been proposed to improve the strength of these plasmon fields: 1) optimization of the structural parameters and materials[1-9], 2) assembly of the plasmonic nanoparticles in

*Corresponding Author. Email: koochaki@aliabadiau.ac.ir

order to create strong coupling interactions between the plasmon fields of neighboring nanoparticles through hybridization[10-15].

In addition to the absorption efficiency, there is another important functional characteristic of meta-material absorbers, called the quality factor (Q-factor) of the resonances. Realization of high Q-factor resonance peaks is a crucial task for realistic applications, like sensing because upon which the resolution is dependent. Besides, in some applications like filtering and optical communications, ultra high Q-factor resonance peaks are highly desirable.

However, most meta-material absorbers provide absorption peaks with low Q-factors due to not only Joule loss but also radiative loss[14, 15]. A simple and effective method to reduce radiative loss of meta-material absorber is to introduce asymmetry into the structure [14-16]. For symmetric nano-structures, only plasmons with finite dipole moments can be excited by the incident optical wave. There are also some invisible modesin the spectrum of the device, known as dark magnetic modes which can become visible via breaking the symmetry of the structure. In fact, this symmetry breaking enables some interactions that render dark magnetic modes dipole active and therefore visible at optical wavelengths[14-16]. The most appealing consequence of this symmetry breaking is the appearance of anti-symmetric resonances, known as Fano resonances, which is associated with a significant increase in the Q-factor of the resonance modes, and extraordinary large plasmon resonance tunability. This higher quality factor stems from the enabled interactions of very narrow dark modes with broad bright modes, via symmetry breaking; and the large tunability is attributed to the high sensitivity of Fano resonances to the changes in the characteristics of the surrounding media such as refractive index, conductivity and so on [11, 17].

To date, several studies have been performed on the engineering of Fano-based meta-material tunable absorbers which mostly consist of non-symmetric periodic structures. An ultra-narrow-band perfect absorber in the near infrared region based on Fano resonances in a MIM meta-material composed of asymmetry double elliptic cylindershas been investigated by Yu *et al*. [14]. Giessen *et al.* showed that coupling strength of plasmon Fano resonances in a metallic photonic crystal can be controlled by varying the thickness of a spacer layer between the gold grating and the waveguide layer[12]. A wide bandwidth plasmonic meta-material absorber containing a broken cross as an elementary cell along with four rectangular loads has been proposed to improve the absorbance and achieve a tunable Fano response [13]. In [15], a crossed ring-shaped meta-surface with highly tunable dual-Fano resonance peaks is proposed and numerically investigated. A Fano-based meta-material absorber consisting of various parasitic elements including cross and L shapes are studied and the functional characteristics of the device are derived for various configurations of the metallic nano-structure [18]. Li *et al.* demonstrated that all dielectric symmetry broken meta-surfaces can provide tunable sharp Fano resonances in their absorption spectrum [16]. The above mentioned studies show that Fano-based meta-material absorbers can offer an effective platform for high performance modulation, sensing, and filtering applications.

In this study, an ultra-narrow bandwidth tunable plasmonic absorber composed of a periodic array of bar antennas with bent arms,deposited on top ofa thin dielectric layer is numerically investigated. We show that non-symmetric plasmonic antennas can provide much larger EM field enhancements than the symmetric structure, due to the appearance of Fano resonances in the absorption spectrum. The dependence of the central wavelength, magnitude and line-width of the absorption peaks upon the structural parameters of the metallic nano-antennas is also investigated. Finally, the influence of adding alayer of graphene on top of the proposed structure, and the dynamic tunability of the optical spectrum under the changes of the chemical potential of the grapheme layer is demonstrated.

The rest of the paper has been arranged as follows. In the next part, the designed structure plus its functional principle have been described and the role of each segment has been expressed. Consecouently, the simulation methodology and the materials will be described. Afterward, the results on the effect of variable geometrical parameters of the proposed nano-antennas on the absorption spectra of the device will be given and discussed. Then, the dynamic tunability of the device including a monolayer graphene will be studied. The simulations at this study

were performed by CST microwave studio software. The summary and conclusion remarks will be given in the last section.

2. Suggested structure and its functional principle

As shown in Figure 1, the suggested structure is a triple-layer (Metal-Insulator-Metal) MIM stack composed of a periodic array of double bar antennas with bent arms, located on top of a silica film. The bottom silver layer acts as a reflector and enhances the absorptivity of the resonance peaks, through blocking the incident field from being transmitted. When illuminating the proposed structure, incident light wave interacts strongly with the meta-surface. This may cause the absorption spectrum of the device to show a few absorption peaks at resonance wavelengths. The central wavelengths, line-widths and peak magnitudes of these resonances are determined by several parameters including size of the bar antennas and their bent arms, the gap size, the dielectric layer thickness, and so forth. Figure 1demonstrates three dimensional and top view schematics of the proposed micro-device. Since the surface of proposed structure is periodic, and the substrate is uniform, the operating principle of a unit cell can be investigated and then generalized to the whole structure.

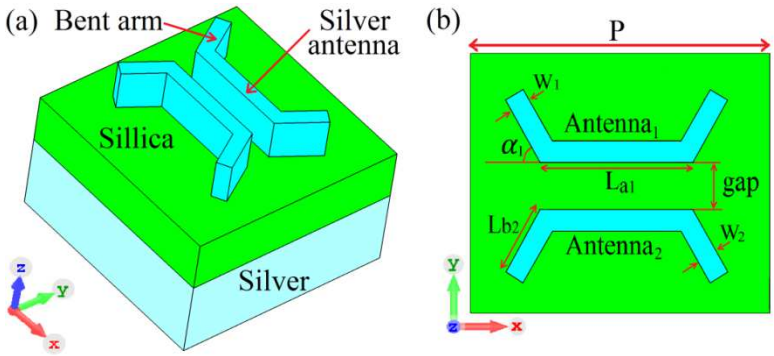

Figure 1: (a) 3D schematic diagram of the proposed meta-material absorber, (b) x-y plane view of the proposed double antenna meta-surface.

Table 1, illustrates the geometrical specifications of a unit cell of the designed absorber. These parameters were taken in a way that the absorption spectrum of the device in the NIR region presents both dipole and Fano resonances.

Table 1: The geometrical specifications of a unit cell of the designed absorber.

Parameters	Symbol	Value
Length of the middle armof antenna$_1$	L_{a1}	220 nm
Length of the middle arm of antenna$_2$	L_{a2}	220 nm
Length of the bent arm of antenaa$_1$	L_{b1}	70 nm
Length of the bent arm of antenaa$_1$	L_{b2}	70 nm
Width of antenna$_1$	W_1	25 nm
Width of antenna$_2$	W_2	25 nm
Length and width of the unit cell	P	450 nm
Thickness of the silver antennas	H_a	65 nm
Thickness of the sillica layer	H_d	350 nm
Thickness of the bottom silver film	H_s	100 nm
Lateral distance between the antennas	gap	30 nm
Bent angle of the bent arm of antenna$_1$	α_1	45°
Bent angle of the bent arm of antenna$_2$	α_2	45◦

3. Simulation method and materials

The suggested structure is numerically analyzed using a frequency domain solver. In the simulations, unit cell boundary conditions are applied for x- and y-coordinates, and open boundary conditions is chosen along the z-axis. A plane wave with electric field (E-field) parallel to the y-axis is radiated on the surface of the unit cell. The absorption spectrum can be calculated by *A=1-R-T* formula; where R and T are the reflectance and transmittance corresponding to$S_{11}$and S_{21}parameters, respectively. When the bottom reflector film exists, S_{21} and consequently T is zero, and the absorption is calculated as *A=1-R*.In the simulations, the relative permittivity of silica is set as 2.25, and The Drude model is used to model the relative permittivity of silver [19, 20]:

$$\varepsilon_m(\omega) = \varepsilon_\infty - \omega_p^2/(\omega^2 + j\gamma\omega)$$

where ω_p, γ and ε_∞ are the plasma frequency, the collision frequency and high frequency relative permittivity of silver which are chosen to be 1.38×10^{16} Hz, 2.37×10^{13} Hz and 3.7, respectively [19].

A 2-D surface conductivity method has been utilized to model the optical response of graphene. In this method, the mono-layer graphene is considered as an ultra-thin film which can be expressed by a complex surface conductivity, σ_g, according to the Kubo formula[21]:

$$\sigma_g = \sigma_g^{inter} + \sigma_g^{intra}, \quad (1)$$

$$\sigma_g^{inter} = -j\frac{e^2 k_B T}{\pi\eta^2(\omega - j2\Gamma)}\left[\frac{\mu_c}{k_B T} + 2\ln\left(\exp\left(-\frac{\mu_c}{k_B T}\right) + 1\right)\right] \quad (2)$$

$$\sigma_g^{intra} = -j\frac{e^2}{4\pi\eta}\ln\left[\frac{2|\mu_c| - \eta(\omega - j2\Gamma)}{2|\mu_c| + \eta(\omega - j2\Gamma)}\right] \quad (3)$$

where σ_g^{intra} and σ_g^{inter} stems from the intra-band and inter-band transitions, respectively. μ_c, Γ, T, k_B, η, and e are, chemical potential of grapheme, scattering rate, temperature, Boltzmann constant, reduced Planck constant, and electron charge, respectively. As a matter of fact, the chemical potential of graphene is dependent upon the density of charge carriers, which can be manually controlled by using avariable voltage power supply. Equation (2) describes the inter-band electro-photon scattering, while Equation (3) represents the intra-band transition contribution. The intra-band contribution is usually approximated for $\eta\omega >> k_B T$ and $|\mu_c| >> k_B T$ [21].We have chosen $\mu_c = 0eV$, $T = 300^\circ\mathrm{K}$, and $\tau = 0.3\,ps$ in our simulations, where $\tau = 1/(2\Gamma)$ is the electron relaxation time in the mono-layer graphene. Besides, the graphene layer thickness is chosen to be0.3 nm throughout the performed simulations.

4. Results and discussion

4.1. Fano resonance in the asymmetric structure

Given the geometrical parameters listed in Table 1, and assuming the structure to be symmetric and there is no reflector film at the bottom of the structure, a single broad-band peak is observed at around $\lambda_d = 870$ nm (black curve in Figure 2(a)), in the reflection spectrum of the proposed absorber. As is expected, by changing the bending angle of one of the antennas (α_1), the structure becomes asymmetric, and an extra resonance peak (at $\lambda_f = 755$ nm)

is appeared in the spectrum due to the Fano resonance phenomenon. This asymmetric Fano peak rises from the interference between quadrupole (dark) and dipole (bright) modes of the metallic structure.

This structure has low absorptivity at Fano resonance because a significant amount of the incident light passes through the structure and does not absorb. By adding a silver layer as a total reflector in the bottom of the structure the Fano resonance becomes much stronger. This is because the reflector layer enhances the interaction between the dark and bright modes. Since the destructive interference between quadrupole and dipole modes suppresses the radiative loss of the metallic structure, the appeared Fano resonance has stronger absorption, narrower bandwidth, and consequently higher Q-factor compared to the dipole bright mode (see Figure 1(b)).

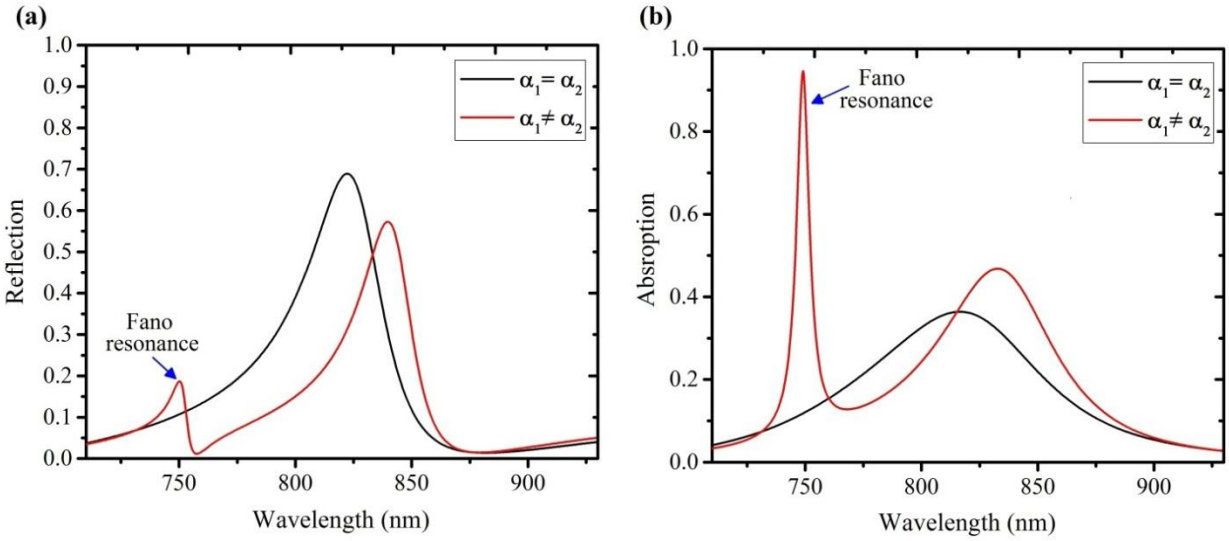

Figure 2: The reflection response of the device illustrated in Figure 1, at the NIR. (a) The absorption spectra of the suggested structure without the bottom reflector layer. (b) The reflection spectra of the suggested structure in the presence of the bottom reflector layer. Black curve: symmetric structure, red curve: asymmetric structure.

To figure out the behavior of R and A spectra depicted in Figure 2, the z component of the E-field at the interface of the dielectric layer and the bar antennas have been investigated and shown in Figure 3. As comes from the figure, for the dipole resonance, the charge distributions around the antennas are the same, though an opposite trend is seen at the quadruple resonance. This implies that, the induced currents are in-phase at the dipole resonance, while they are anti-phase at the quadruple resonance. The interference between the quadruple and dipole modes with anti-phase oscillations results in a very trivial radiative loss at the pertinent wavelength and an ultra-narrow resonance peak (named Fano resonance) emerges.

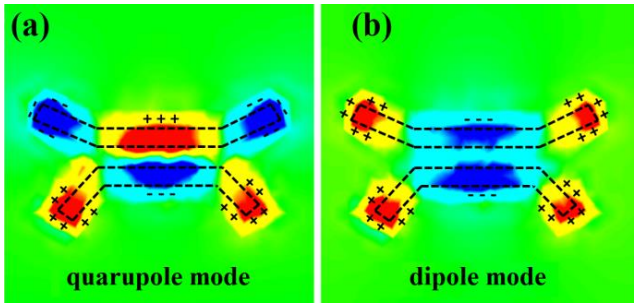

Figure 3: z component of the E-field distribution at the interface between dielectric layer and the metallic antennas. (a) $E_z$at the quadrupole resonance ($\lambda_f = 750$ nm); (b) E_z at the dipole resonance ($\lambda_d = 870$ nm).

4.2. The influence of geometrical parameters

As discussed before, the structural asymmetry is the main reason behind the appearance of the Fano resonance in the absorption spectra of the presented structure. This asymmetry can be easily induced and adjusted by changing the bending angle of one of the antennas while that of the other one is fixed. The influence of the changes in α_1 on the Fano resonance, while $\alpha_2 = 45^\circ$ is shown in Figure 4. The other structural parameters are considered to be constant as listed in Table 1.

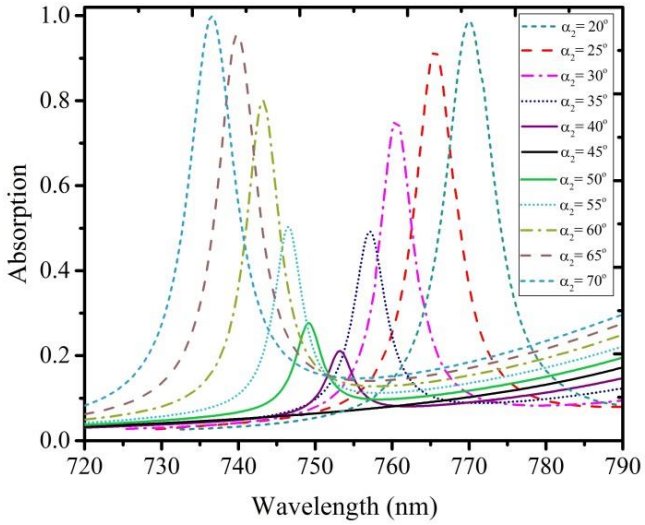

Figure 4: The absorption spectrum of the suggested structure at around Fano resonance for various amounts of α_1, while α_2 is fixed at 45° and the other structural parameters are unchanged.

One can understand from the figure that when α_1 is not equal to $\alpha_2 = 45^\circ$, a narrowband Fano resonance peak is appeared in the spectrum at around 755 nm. Moreover, for $\alpha_1 > 45^\circ$, when α_1 becomes larger, the Fano peak is blue shifted and its magnitude becomes larger until it gets near 100%. By contrast, for $\alpha_1 < 45^\circ$, as α_1 becomes smaller, the Fano peak experiences a red shift and its magnitude becomes larger. In other words, the magnitude of the Fano resonance increases with the increase of asymmetry, because enlarging the value of α strengthens the excitation of localized plasmons of the dark quadrupole mode.

An important parameter usually considered in the design of resonant devices is the Q-factor of the resonance peaks that is defined as:

$$Q = \frac{\text{FWHM}}{\lambda_f},$$

whereFWHM is the full width at half maximum of the Fano resonance peak, and λ_f is its central wavelength. From Figure 4, one can say that as the difference between α_1 and α_2 gets larger (i.e., the degree of asymmetry increases), the line-width of the Fano peak is increased, and its Q-factor is therefore decreased. This can be explained according to a general fact: the Fano resonance Q-factor and the degree of asymmetry of the structure are inversely related. This general fact can be described by the phenomenon of bound states in the continuum, originating from quantum mechanics as an important physical concept of destructive interference [16].

Another way to introduce asymmetry into the proposed structure and inducing Fano resonance is to rotate one of the antennas while the other on is fixed (see Figure 5). In this case, we expect to see an extra Fano peak in the absorption spectrum of the proposed micro device. Figure 6 illustrates the optical response of the proposed device to the changes of the rotation angle, θ_1.

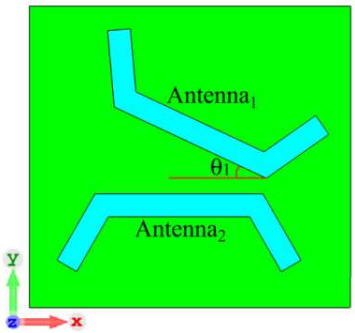

Figure 5: In plane rotation of antenna number 1, while antenna number 2 is fixed in its initial position.

According to Figure 6, when $\theta_1 > 0°$, another Fano peak is appeared at around $1550\ nm$ in addition to the Fano peak related to the difference between α_1 and α_2, which was appeared at around 755 nm. Here, the Fano peak appeared at 755 nm is called the1stFano peak, and the peak at 1550 nm is called the 2ndFano peak. As can be seen in the inset of Figure 6, increasing the angle of rotation increases the absorptivity of the 2ndFano peak, and shifts it towards longer wavelengths. We can also learn from the figure that, the changes of rotation angle have negligible effect on the absorptivity and central wavelength of the 1stFano peak.

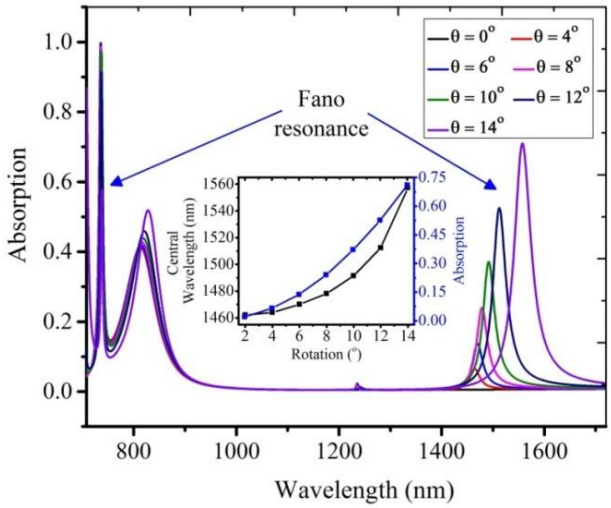

Figure 6: The influence of rotation angle on the absorption spectrum of the proposed device when $\alpha_1 = 45$, $\alpha_2 = 70$, and other parameters are constant as listed in Table 1. The inset shows the central wavelength and absorptivity of the 2ndFanopeak as a function of rotation angle.

Owing to the fact that the intensity of the EM radiation is confined and enhanced in the gap between adjacent antennas at quadruple resonance, induced by the anti-phase oscillations of quadruple mode, the size of the gap strongly affects the Fano resonance characteristics. The behavior of the absorption spectrum of the proposed absorber for various values of gap size is shown in Figure 7. It is expected that by making the gap smaller, the intensity of interaction between asymmetric bars to be increased, resulting in an increase in the value of Q-factor of the Fano resonance peak. This can be seen in the inset of Figure 7. From this figure, one can also see that the smaller gap results in a significant blue shift of the dipole resonance, but negligible red shift of the Fano resonance peak.

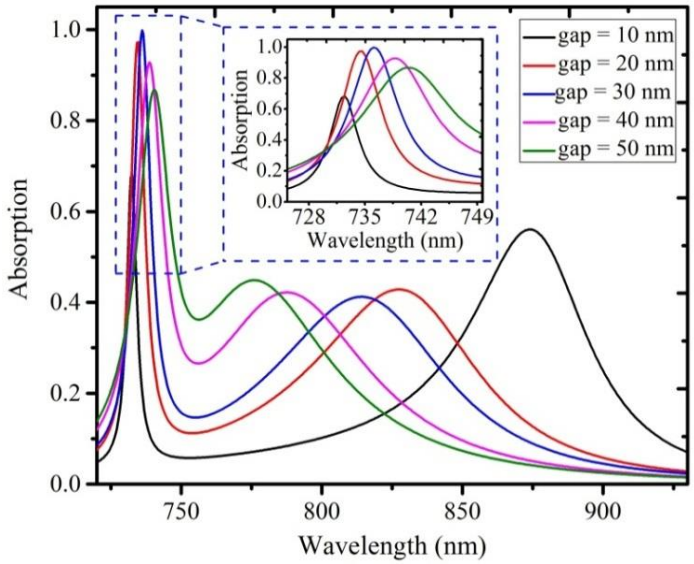

Figure 7: The absorption spectra of the suggested device for various values of the gap width from 10 nm to 50 nm. The inset shows a magnification of the Fano peak.

As discussed before, Q-factor of the Fano peak is one of the most important parameters of the proposed structure, and the simplest way to increase it, is to decrease the degree of asymmetry[16].This can be done by decreasing the length of bent arms of the antennas. Figure 8 illustrates the behavior of the absorption spectrum for different amounts of bent arm length of the antennas, $L_{b1}$and L_{b2}. As illustrated in Figure 8, the reduction ofL_{b1} and L_{b2} leads to a blue shift of the Fano resonance peak and a significant increase of its Q-factor. The inset shows that for$L_b = L_{b1} = L_{b2} = 40$ nm, the Fano resonance peak with a Q-factor of 387 (corresponding to a FWHM of 1.83 nm) is appeared at 710 nm. The figure also depicts that further decrease of $L_{b2}$and L_{b1} results in the increase of dipole resonance magnitude but reduction of Fano peak absorptivity which is undesirable.

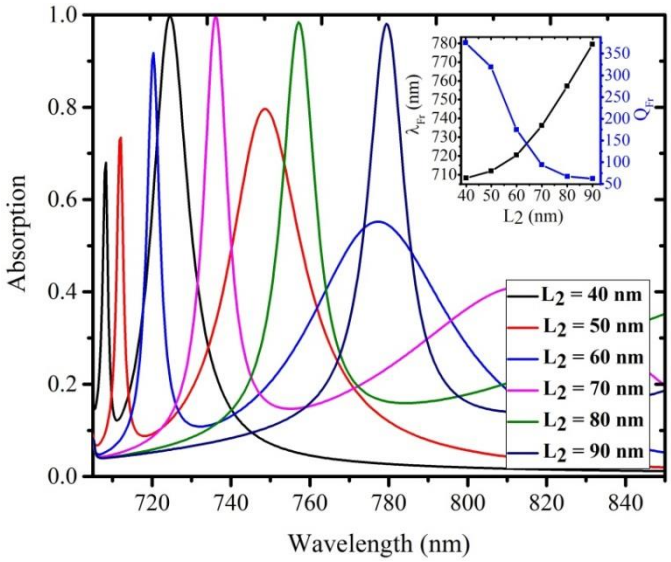

Figure 8: The effect of bent arms' length L_b on the absorption spectra of the proposed absorber. The inset shows the relationship between L_b and Fano peak central wavelength as well as its absorptivity.

There are also other geometrical parameters, like antennas' width (W_a) and height (H_a),that strongly affect the absorption spectrum of the designed device. The influences of H_a and W_a on the spectrum of the device are

illustrated in Figure 9 and Figure 10, respectively. Investigation of these figures reveals that, the central wavelength of the Fano peak experiences an exponential blue shift with the increase of W_a or H_a. It is also interpreted form these figures that, the increase of W_a or H_a results in a reduction in the difference between the central wavelength of Fano and dipole peaks.

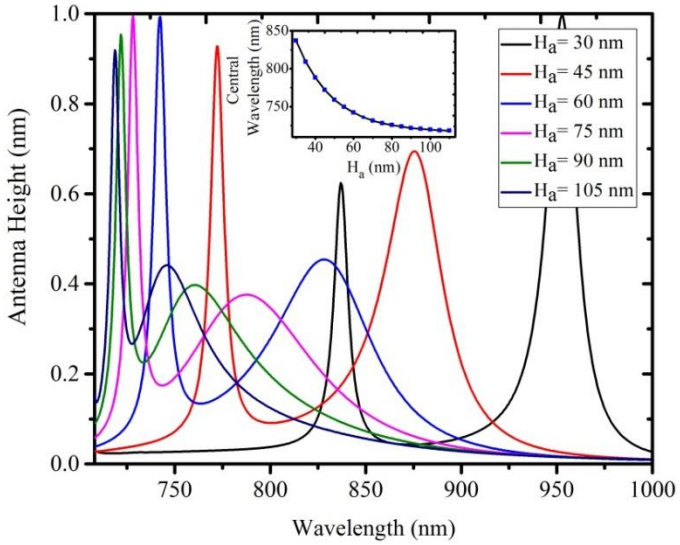

Figure 9: The influence of the antennas' height on the optical spectrum of the device. The inset shows the central wavelength of the Fano resonance versus H_a.

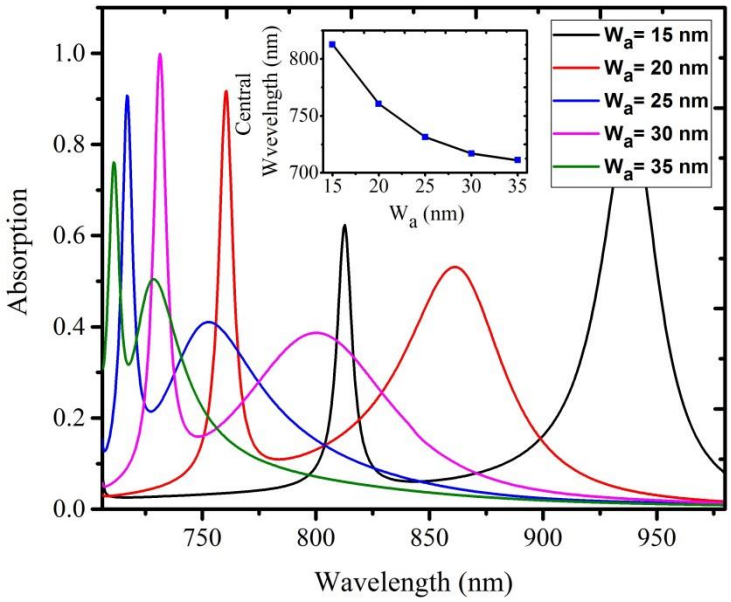

Figure 10: The influence of the antennas' width on the optical spectrum of the device. The inset shows the central wavelength of the Fano resonance as a function of W_a.

4.3. Dynamic tunability using a single layer graphene

There are a lot of methods used to realize dynamically tunable optical absorbers and modulators among which electrical excitation using graphene is the most popular one thanks to its unique electrical and optical features. The most prominent optical characteristic of graphene is the flat absorption spectrum that can be tuned by applying an external E-field. This property can enable the tunability of surface conductivity through alteration of its Fermi energy. Meanwhile, the premium high carrier mobility of graphene (~23000 $cm^2/V.s$ for top gated graphene) makes it an appropriate choice for ultrafast optoelectronic applications. Nevertheless, graphene possesses a very low optical absorption (2.3% for a single layer of suspended graphene), However, using graphene in combination with plasmonic devices can make up for this disadvantage. It means that, since graphene shows strong coupling with enhanced EM field in the plasmonic structures, it is possible to realize highly tunable devices with this material. In this section, the consequences of adding a layer of graphene to the structure of the proposed absorber are investigated. Figure 11 shows the 3D schematic of the proposed absorber with a graphene layer added to the structure on top of the silica sheet. As a general fact, the EM field enhancement around the metallic antennas interacts strongly with the graphene layer, resulting in an efficient improvement of the graphene influence on the optical behavior of the device.

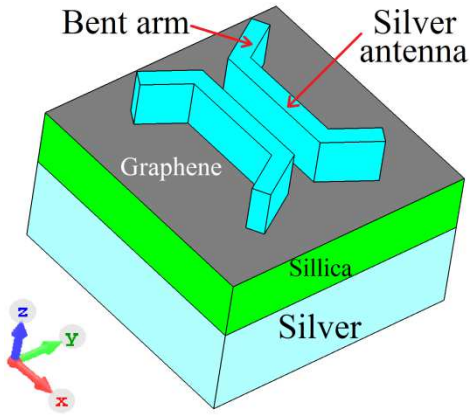

Figure 11: 3D schematic of the proposed structure with a mono-layer graphene between the metallic antenna and the silica layer.

To describe the influence of graphene on the absorption spectrum of the designed meta-surface, the absorption spectra with and without graphene layer has been shown comparatively in Figure 12. As shown in this figure, without graphene, the absorption related to the Fano and dipole resonance peaks are around 99% and 40%, respectively. However, with graphene layer (EF=0 eV), the absorption related to the Fano peak falls down to 65%, while that of the dipole peak rises to 95%. Indeed, the increase observed in the absorptivity of the dipole resonance comes from the constant absorption of graphene in the NIR that is now strengthen owing to the intense increase of the EM field on the surface stemming from the excitation of the localized surface plasmons (LSPs). However, the decreased value of Fano resonance peak in the presence of graphene and the different reactions of Fano and dipole modes to the existence of the graphene layer can be explained by investigating the E-field and charge distributions around the antennas at the quadrupole and dipole resonances. According to Figure 3(a), for the Fano resonance, a large amount of opposite charges is accumulated in the gap between the antennas. Once the gap is occupied with graphene, the opposite charges are recombined and neutralized via the highly conductive graphene layer, resulting in a strong suppression of the E-field enhancement[22].Hence, the magnitude and Q-factor of the Fano resonance peak are decreases significantly. This is while, as illustrated in Figure 3(b), for the dipole mode, a vertically symmetric distribution of charges is observed in the gap. Since the graphene layer does not affect the accumulation of the same type of charges, no EM field suppression is expected in the presence of graphene at the dipole mode. So, the

absorptivity in this wavelength is only influenced by the enhancement of the absorption of graphene due to the excitation of LSP resonances.

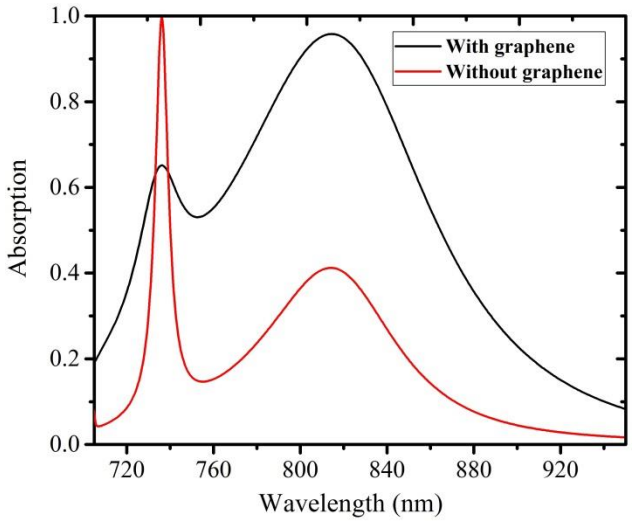

Figure 12: The absorption spectra of the device with and without the mono-layer graphene.

As discussed before, the hybridization of graphene with meta-material structures enables the active tunability of the optical spectrum by manipulating the Fermi level of graphene via applying a variable voltage source. Figure 13 (a) exhibits the absorption spectrum of the device under the variations ofthe graphene chemical potential. It is seen that as the chemical potential increases from 0.7 to 0.9 eV, the absorptivity of the dipole resonance drops by about 55%, corresponding to -275%/eV modulation of absorptivity per graphene Fermi energy (Figure 13b). Morever, the decrease in absorptivity initiated at EF=0.7eV and ended at EF=0.9 eV. The decrease in absorptivity at the indicated range can be assigned to the decrease in the grapheme. Detailed description of this phenomenon is discussed in other similar contributions[9].

On the other hand, as depicted in Figure 13a, the absorptivity of the Fano peak increases with the increase of the chemical potential. From Figure 13b, the absorptivity of the Fano peak changes from 0.65 to 0.99 as EF increases from 0.8 to 0.95 eV. Hence, a tunability of 226%/eV can be achieved for the Fano peak. It is worth mentioning that the absorption spectrum of the device for $E_f = 0.95$ eV is the same as that of the device without the graphene layer. This is because, at $E_f = 0.95$ eV the conductivity of the graphene layer is nearly zero, and thus there is no effect on the Fano peak. On the other hand, for $E_f = 0.95$ eV, the absorption of the monolayer graphene tends to zero and therefore the graphene layer has no impact on the absorptivity of the dipole mode. Moreover, as shown in the inset of Figure 13(a), a negligible red shift of the Fano peak under the variations of the chemical potential of graphene is observed which can be attributed the changes of effective refractive index of the surrounding media due to the changes in refractive index of the graphene layer.

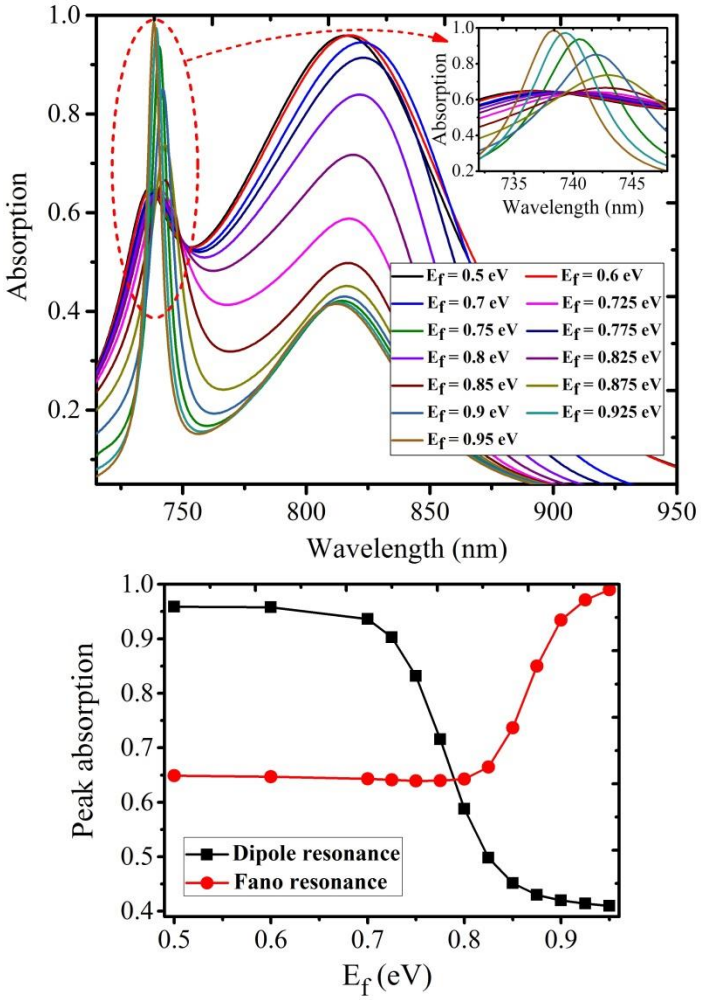

Figure 13: The effect of variations of graphene chemical potential on the optical response of the device. (a)Absorption spectra of the deviceunder the variations of the Fermi energy, while the other parameters are fixed as listed in Table 1; (b) Absorptivity of the Fano and dipole peaks as a function of the Fermi energy of the graphene.

Unlike the dipole resonance, the changes in the absorptivity of the Fano peak due to the variations of the Fermi energy, stems from the changes in the conductivity of the graphene layer not its absorption. As mentioned before, the surface conductivity of the graphene layer leads to the neutralization of opposite charges in the gap between the metallic antennas, resulting in a reduction in the absorptivity of the Fano peak. Therefore, it is easy to say that, the more the surface conductivity of graphene is, the less the absorptivity of the Fano peak gets, and vice versa. To investigate the behavior of the surface conductivity under the variations of the chemical potential, the real part of surface conductivity for various values of E_f is calculated as depicted in Figure 14. It is clear for this figure that for a certain wavelength (e.g., the Fano resonance at 730 nm), the surface conductivity of graphene is decreased by the increase of chemical potential. Therefore, the recombination and neutralization of the accumulated charges in the gap are limited, resulting in lesser suppression of the E-field enhancement.

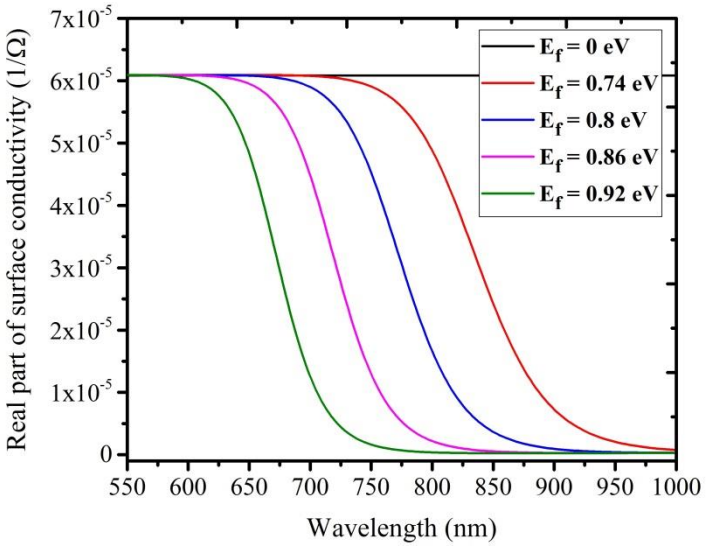

Figure 14: response of the surface conductivity of graphene to the variations of the Fermi energy from 0 to 0.92 eV.

According to the above discussion, the proposed structure can be utilized as a highly tunable optical modulator with anultra-narrow band (7.8 nm line-width) channel and a broad band (100 nm line-width) channel, which behave oppositely.

5. Conclusion

In summary, the absorption response of a MIM plasmonic structure, including a dielectric layer sandwiched between asymmetric double metallic antennas and a metallic filmhas been numerically investigated. Results revealed that, in addition to the dipole peak, two individual Fano peaks emerged in the spectrum as two structural asymmetry factors were applied simultaneously. Furthermore, an ultra-narrow band resonance peak with a bandwidth of 1.87 nm at the wavelength of 710 nm (corresponding to a Q-factor of 387) was obtained by controlling the geometrical parameters. The variation of the absorption spectrum in the presence of an extra layer of grpahene has also been surveyed. Since the surface conductivity of graphene is controllable via changing the chemical potential, the observed Fano and dipole peaks were dynamically tunable by applying a variable gate voltage. Modulation of absorption per graphene Fermi energy of -275 %/eV and 226 %/eV has been obtained, respectively, for the Fano and dipole peaks. According to the mentioned characteristics, the suggested device can be utilized in a broad range of applications such as tunable reflectors and photo-detectors and optical modulators.

Funding

No funds, grants, or other support was received.

Conflicts of interest/Competing interests

The authors declare that they have no known competing financial interests or personal relationships that could have appeared to influence the work reported in this paper.

Availability of data and material

Data will be made available on reasonable request.

Code availability

Simulation results will be made available on reasonable request.

Authors' contributions

All authors contributed to the study conception and design. Material preparation, data collection and analysis were performed by Aliakbar Mashkour, Amangaldi Koochaki , Ali Abdolahzadeh Ziabari, and Azadeh Sadat

Naeimi. The first draft of the manuscript was written by Aliakbar Mashkour and all authors commented on previous versions of the manuscript. All authors read and approved the final manuscript.

Ethics approval

There are not any human participants, their data or biological material in this study.

Not applicable.

Consent to participate

Not applicable.

Consent for publication

Not applicable.

References:

[1] R. K. Jaiswal, N. Pandit, and N. P. Pathak, "Center Frequency and Bandwidth Reconfigurable Spoof Surface Plasmonic Metamaterial Band-Pass Filter," *Plasmonics,* vol. 14, pp. 1539-1546, 2019.

[2] Y. Yang, Y. Xu, B. Zhang, J. Duan, L. Yan, H. Xu*, et al.*, "Investigating flexible band-stop metamaterial filter over THz," *Optics Communications,* vol. 438, pp. 39-45, 2019.

[3] Y. Fan, Y. Qian, S. Yin, D. Li, M. Jiang, X. Lin*, et al.*, "Multi-band tunable terahertz bandpass filter based on vanadium dioxide hybrid metamaterial," *Materials Research Express,* vol. 6, p. 055809, 2019.

[4] Z. Vafapour, "Polarization-independent perfect optical metamaterial absorber as a glucose sensor in Food Industry applications," *IEEE transactions on nanobioscience,* vol. 18, pp. 622-627, 2019.

[5] A. Lochbaum, A. Dorodnyy, U. Koch, S. M. Koepfli, S. Volk, Y. Fedoryshyn*, et al.*, "Compact Mid-Infrared Gas Sensing Enabled by an All-Metamaterial Design," *Nano Letters,* vol. 20, pp. 4169-4176, 2020.

[6] K. Wang, H. Hu, S. Lu, M. Jin, Y. Wang, and T. He, "Visible and near-infrared dual-band photodetector based on gold–silicon metamaterial," *Applied Physics Letters,* vol. 116, p. 203107, 2020.

[7] A. Ahmadivand, B. Gerislioglu, and Z. Ramezani, "Generation of magnetoelectric photocurrents using toroidal resonances: a new class of infrared plasmonic photodetectors," *Nanoscale,* vol. 11, pp. 13108-13116, 2019.

[8] M. Oshita, H. Takahashi, Y. Ajiki, and T. Kan, "Reconfigurable Surface Plasmon Resonance Photodetector with a MEMS Deformable Cantilever," *ACS Photonics,* vol. 7, pp. 673-679, 2020.

[9] B. Beiranvand, A. S. Sobolev, and A. Sheikhaleh, "A proposal for a dual-band tunable plasmonic absorber using concentric-rings resonators and mono-layer graphene," *Optik,* vol. 223, p. 165587, 2020.

[10] R. Kumar and S. A. Ramakrishna, "Simple trilayer metamaterial absorber associated with Fano-like resonance," *Journal of Nanophotonics,* vol. 14, p. 016011, 2020.

[11] Z. He, W. Xue, W. Cui, C. Li, Z. Li, L. Pu*, et al.*, "Tunable Fano Resonance and Enhanced Sensing in a Simple Au/TiO2 Hybrid Metasurface," *Nanomaterials,* vol. 10, p. 687, 2020.

[12] C. Bauer and H. Giessen, "Tailoring the plasmonic Fano resonance in metallic photonic crystals," *Nanophotonics,* vol. 9, pp. 523-531, 2020.

[13] M. R. Soheilifar, "Wideband optical absorber based on plasmonic metamaterial cross structure," *Optical and Quantum Electronics,* vol. 50, p. 442, 2018.

[14] M. Zhang, J. Fang, F. Zhang, J. Chen, and H. Yu, "Ultra-narrow band perfect absorbers based on Fano resonance in MIM metamaterials," *Optics Communications,* vol. 405, pp. 216-221, 2017.

[15] Z. He, C. Li, W. Cui, W. Xue, Z. Li, L. Pu*, et al.*, "Dual-Fano resonances and sensing properties in the crossed ring-shaped metasurface," *Results in Physics,* p. 103140, 2020.

[16] X. Long, M. Zhang, Z. Xie, M. Tang, and L. Li, "Sharp Fano resonance induced by all-dielectric asymmetric metasurface," *Optics Communications,* vol. 459, p. 124942, 2020.

[17] M. H. Elshorbagy, A. Cuadrado, G. González, F. J. González, and J. Alda, "Performance improvement of refractometric sensors through hybrid plasmonic–fano resonances," *Journal of Lightwave Technology,* vol. 37, pp. 2905-2913, 2019.

[18] F. Tavakoli, F. B. Zarrabi, and H. Saghaei, "Modeling and analysis of high-sensitivity refractive index sensors based on plasmonic absorbers with Fano response in the near-infrared spectral region," *Applied optics,* vol. 58, pp. 5404-5414, 2019.

[19] P. B. Johnson and R.-W. Christy, "Optical constants of the noble metals," *Physical review B,* vol. 6, p. 4370, 1972.

[20] I. H. Malitson, "Interspecimen comparison of the refractive index of fused silica," *Josa,* vol. 55, pp. 1205-1209, 1965.

[21] G. W. Hanson, "Dyadic Green's functions and guided surface waves for a surface conductivity model of graphene," *Journal of Applied Physics,* vol. 103, p. 064302, 2008.

[22] S. Xiao, T. Wang, X. Jiang, X. Yan, L. Cheng, B. Wang*, et al.*, "Strong interaction between graphene layer and Fano resonance in terahertz metamaterials," *Journal of Physics D: Applied Physics,* vol. 50, p. 195101, 2017/04/13 2017.